Reversible mechanism for spin crossover in transition-metal cyanides

Mukul Kabir and Krystyn J. Van Vliet

Reversible mechanism for spin crossover in transition-metal cyanides

Mukul Kabir and Krystyn J. Van Vliet

Department of Materials Science and Engineering,
Massachusetts Institute of Technology, Cambridge, Massachusetts 02139, USA

(Dated: February 15, 2012)

We report the mechanisms for reversible and repeatable spin transition in a Prussian blue analog crystal, $KCo[Fe(CN)_6]$, derived from first-principles calculations. The forward and reverse transitions are initiated by metal-to-metal charge transfer, followed by the d-electron rearrangement at the Co center. Further, these transitions are strongly correlated with bond lengths within the crystal lattice. Both aspects of this spin crossover are in quantitative agreement with experiments. Moreover, we find that the presence of H_2O molecules within this Prussian blue analog crystal is not essential to trigger spin transitions in such materials.

I. INTRODUCTION

Spin crossover generally occurs in octahedrally coordinated $3d$ transition metal complexes, and can be induced by external perturbations in various forms[1–10] by tuning the competing intra-atomic exchange energy (Hund's coupling), and the crystal field energy. Such spin transitions are observed in molecular-based magnets,[1–5] oxides,[6–8] supra-molecular systems,[9] and metal-organic complexes,[11] which show promising application capabilities in sensors, switches, and recording devices.

Photoinduced spin transitions was first observed in the cobalt-iron Prussian blue analog (CoFe-PBA), $K_{0.2}Co_{1.4}[Fe(CN)_6]\cdot6.9H_2O$ at temperatures below 20 K. Illumination with visible light at low temperature induces bulk magnetization, which can be eliminated by near-infrared light.[1,2] This entire process is repeatable. It is believed that the spin transition in CoFe-PBA at low temperature occurs due to the existence of a long-lived metastable high spin (HS) excited state $[Fe^{III}(t_{2g}^5;\ S=1/2)-CN-Co^{II}(t_{2g}^5e_g^2;\ S=3/2)]$ at low energy above the low spin (LS) ground state $[Fe^{II}(t_{2g}^6;\ S=0)-CN-Co^{III}(t_{2g}^6;\ S=0)]$, which can be reversibly populated by visible and near-IR light, respectively.[1,2] Experiments have demonstrated that these transitions are also strongly coupled with the internal PBA lattice via the volume change in the CoN_6 octahedra.[12,13] The global phase transitions in both directions are also believed to be triggered by metal-to-metal charge transfer (CT) excitations,[14] rather than the photogenerated polarons which have been observed in other compounds.[15]

The structural parameters and the local electronic configurations of both the LS ground state and HS metastable excited states are well characterized for CoFe-PBA.[1,2,12,13] However, neither the microscopic transition mechanisms nor the effects of Fe-vacancies, water, and alkali metals on these mechanisms are completely understood, despite considerable experimental and theoretical effort.[16–19] Similar spin crossover has been also observed in other Prussian blue analogues such as $RbMn[Fe(CN)_6]$ (Ref.[20]) and $CsFe[Cr(CN)_6]$ (Ref.[21,22]), and Wojdeł has

shown that intrinsic H_2O in the Prussian blue crystal $KFe[Fe(CN)_6]$ does not influence the charge transfer excitation energy.[23]

Here we investigate the microscopic spin transition mechanisms via an *ab initio* lattice model for CoFe-PBA. We find that the forward and reverse spin transitions are indeed triggered by metal-to-metal CT excitations. The forward transition is mediated via tetragonal Jahn-Teller (JT) distortion of the CoN_6 octahedra, which is not the case for the reverse transition. Moreover, as this spin crossover is realized in the anhydrous form of this crystal, we find that incorporated H_2O molecules are not essential prerequisites of the transition as had been proposed previously.[19]

II. COMPUTATIONAL METHODS

We conducted density functional theory (DFT) calculations of the dehydrated PBA crystal as schematized
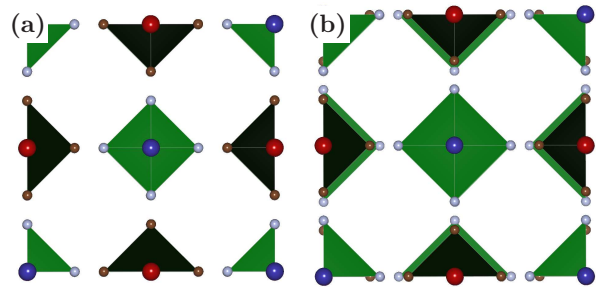

FIG. 1. (Color online) Similar to the Prussian blue family of mixed-metal poly-cyanides, the CoFe-PBA exhibits a face-centered cubic (fcc) structure comprising a three-dimensional network of CoN_6 (green) and FeC_6 (black) octahedra. The major structural difference between the (a) low-spin and (b) high-spin states lies in the Co-N bond length, which is ∼0.21 Å longer in the high-spin state (Table I). Atomic elements are shaded as follows: Co (blue), Fe (red); N (gray); and C (brown). Alkali metal cations (K^+) occupy the tetrahedral sites of the fcc structure, and are not shown for clarity.

TABLE I. The PBE functional underestimates both lattice parameter a and band gap E_g, whereas the hybrid PBE0 functional substantially overestimates E_g. In contrast, experimental structural parameters,[12,13] and band gaps[1,2] are well reproduced within the PBE + U ($U_{\mathrm{Co/Fe}}^{\mathrm{eff}} = 3$ eV) approach. See text for justification of this magnitude of U. $\delta d_{\mathrm{Co-N}}$ is the difference in the Co-N bond length for HS and LS states, and ΔE_{LH} [$= E(\mathrm{LS}) - E(\mathrm{HS})$] is the difference in free energy per formula unit (fu).

	LS: $\mathrm{Fe^{II}}(S=0)$-CN-$\mathrm{Co^{III}}(S=0)$					HS: $\mathrm{Fe^{III}}(S=1/2)$-CN-$\mathrm{Co^{II}}(S=3/2)$					$\delta d_{\mathrm{Co-N}}$	ΔE_{LH}
	a (Å)	$d_{\mathrm{Fe-C}}$	$d_{\mathrm{Co-N}}$	$d_{\mathrm{C-N}}$	E_{g} (eV)	a (Å)	$d_{\mathrm{Fe-C}}$	$d_{\mathrm{Co-N}}$	$d_{\mathrm{C-N}}$	E_{g} (eV)	(Å)	(eV/fu)
PBE	9.87	1.88	1.88	1.17	1.30	10.23	1.89	2.05	1.17	1.55	0.17	-1.25
PBE0	9.83	1.88	1.87	1.16	4.52	10.27	1.90	2.08	1.16	2.53	0.21	-0.20
PBE + U	9.92	1.89	1.89	1.17	2.08	10.39	1.92	2.10	1.17	1.25	0.21	-0.18
Exp.	9.96 ± 0.06	1.93	1.91	1.13	~ 2.25	10.36 ± 0.06	1.93	2.11	1.13	~ 0.94	0.20	—

in Fig. 1. We used the Perdew-Burke-Ernzerhof (PBE) exchange-correlation functional,[24] and projector augmented wave pseudopotential[25] as implemented in the VASP code.[26,27] The total electronic energies were evaluated at a kinetic energy cutoff of 500 eV, with 4×4×4 Monkhorst-Pack k-points. Symmetry unrestricted structural relaxations were performed until the Hellmann-Feynman forces were less than 0.01 eV/Å.

III. RESULTS AND DISCUSSIONS

For PBAs, the failure of conventional DFT calculations are manifested via substantial underestimation of the lattice constant and band gap for both LS and HS states (Table I). This is attributed to the insufficient description of electronic self-interaction in the PBE exchange-correlation functional. In contrast, the hybrid PBE0 functional[28] underestimates the lattice parameter and substantially overestimates the band gap (Table I).[29] The amount of $E_{\mathrm{x}}^{\mathrm{HF}}$ mixing in the PBE0 functional substantially alters the band gap, while the lattice parameter does not show such dependence. A hybrid functional with 8% $E_{\mathrm{x}}^{\mathrm{HF}}$ (92% $E_{\mathrm{x}}^{\mathrm{PBE}}$) reasonably reproduces the experimental band gap.

Alternative modifications of the exchange-correlation functional include the Hubbard U parameter (PBE + U). We adopted this tractable approximation and determined the magnitude of U as that which most closely reproduced the experimentally measured structural and electronic properties of this CoFe-PBA crystal. We find that $U_{\mathrm{Co/Fe}}^{\mathrm{eff}} = 3$ eV predicts the LS and HS state of the crystal to be the ground state and the first metastable excited state, respectively, at 0K, which is in agreement with experimental results.[1,2,12,13] $U_{\mathrm{Co/Fe}}^{\mathrm{eff}} = 3$ eV also reproduces the corresponding experimental structural and electronic properties of these magnetic structures (Table I).[1,2,12,13] Further, this correspondence is not critically sensitive to variation in $U \pm 10\%$ about 3 eV. However, any variation beyond $\pm 10\%$ does not well reproduce the experimental electronic and magnetic properties of this PBA crystal. For example, $U_{\mathrm{co/Fe}}^{\mathrm{eff}} \geqslant 3.5$ eV wrongly alters the relative stability of LS and HS states at 0K, where the HS state becomes lower in energy.

Note that we find the $\mathrm{Fe^{II}}$ in CoFe-PBA to be in the low spin ($S = 0$) state, which is in contrast to other complex compounds such as (Mg, Fe)O and (Mg, Fe)$\mathrm{SiO_3}$ (Ref.[6–8]) for which $\mathrm{Fe^{II}}$ exhibits a high-spin ($S = 2$) configuration at ambient pressure. In fact, for CoFe-PBA, the high-spin $\mathrm{Fe^{II}}$ is of significantly higher energy (1.94 eV/fu) than the LS-$\mathrm{Fe^{II}}(S = 0)$. We also find that other possible high-spin structures, $\mathrm{Fe^{III}}(S = 3/2)$-CN-$\mathrm{Co^{II}}(S = 3/2)$ and $\mathrm{Fe^{III}}(S = 5/2)$-CN-$\mathrm{Co^{II}}(S = 3/2)$, are much higher in energy (1.16 and 1.85 eV/fu, respectively) compared to the HS state reported in Table I.

Calculated structural parameters for both the spin states are in excellent agreement with experimental K-edge extended x-ray absorption fine-structure spectroscopy (Table I).[12,13] The free energy difference ΔE_{LH} is only 0.18 eV/fu. Although we are aware of no explicit experimental measurement of ΔE_{LH}, Liu et al. reported laser induced phase transitions at high temperature ($T > 165$ K) and concluded that the HS (high T) and LS (low T) phases were close in energy.[14]

The octahedral coordination of Fe and Co (Fig. 1) splits the respective d-manifold into t_{2g} and e_g levels. Figure 2 shows that in the LS (HS) state, Co-e_g^* (Fe-t_{2g}^*) forms the conduction band ($E - E_F > 0$), whereas Fe-t_{2g} (Co-t_{2g}) forms the valence band. Thus, the d-projected local density of states in both LS and HS states shows the metal-to-metal charge transfer character (Fig. 2) in agreement with experimental absorption spectra.[1,2,30] Further, the calculated CT excitation Fe-$t_{2g} \to$ Co-e_g^* for the LS state (2.08 eV) well predicts the experimental absorption peak observed at ∼550 nm (2.25 eV).[1,2,30] The Co-t_{2g} states lie 1.3 eV below the Fermi level and show a significant mixing with p states of N, whereas the Co-e_g^* states lie 2.08 eV above the Fermi level. These represent $\mathrm{Fe^{II}}$ and $\mathrm{Co^{III}}$ oxidation states, which are in agreement with x-ray absorption spectroscopy results.[12,13] Calculated octahedral crystal field splitting is very high for both Co and Fe ($\Delta_{\mathrm{o}}^{\mathrm{Fe}} = 4.77$ eV and $\Delta_{\mathrm{o}}^{\mathrm{Co}} = 3.40$ eV), and thus both $\mathrm{Fe^{II}}(t_{2g}^6 e_g^0)$ and $\mathrm{Co^{III}}(t_{2g}^6 e_g^0)$ exhibit LS configurations (Fig. 2). These calculated octahedral splittings are in reasonable agreement with those predicted via experimental $L_{2,3}$-edge x-ray absorption spectra for a similar PBA, RbCoFe ($\Delta_{\mathrm{o}}^{\mathrm{Fe}} = 4.2$ eV and $\Delta_{\mathrm{o}}^{\mathrm{Co}} = 2.40\text{-}2.70$
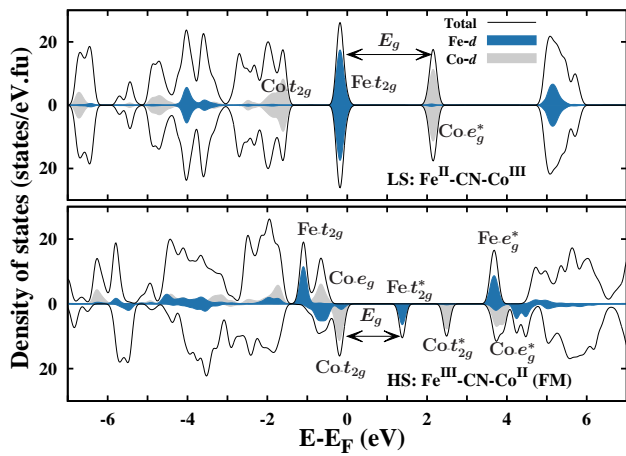
FIG. 2. (Color online) Density of states in forward and reverse spin transitions indicates metal-to-metal charge transfer. The valence band of the low-spin (high-spin) state is composed with the Fe-t_{2g} (Co-t_{2g}) states, whereas the conduction band is composed with the Co-e_g (Fe-t_{2g}) states. Calculated charge transfer excitations agree with the experimental absorption spectra.[1,2,30]
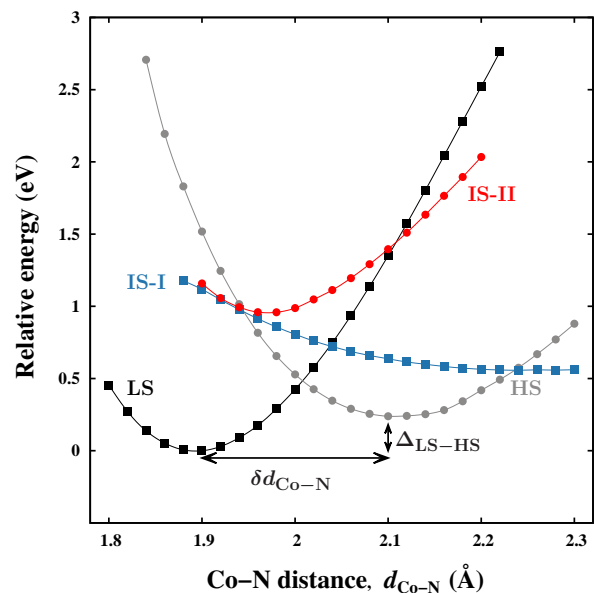

FIG. 3. (Color online) Electronic transitions are strongly coupled with the structural relaxations of the CoN$_6$-octahedra. The CoN$_6$ octahedra of the PBA crystal are elongated along the Co-N ligands by a distance δd_{Co-N} in the high-spin state. Thus, we calculate the relative free energy ($E - E_{LS}$) at varying d_{Co-N} for different spin states. The forward and reverse spin transitions are both mediated via intermediate states.

eV).[16,31,32]

For the ferromagnetic (FM) high spin state, the band gap energy of 1.25 eV in the minority spin channel represents the Co^{II} →Fe^{III} CT excitation (Fig. 2). These findings are in agreement with the experimental CT peak at 1319 nm (0.94 eV).[1,2] The calculated Co crystal field splitting (Δ_o^{Co}=0.97 eV) also agrees with x-ray absorption spectra (1.1 eV).[16,31,32] There is a further splitting between the majority and minority spin channels due to intra-atomic exchange interaction. If this exchange splitting Δ_x is higher than Δ_o, the majority spin channel is occupied first, followed by minority spin channel. As a result, the atom is in the HS state. For Co, the Δ_x (1.35 eV) is higher than Δ_o (0.97 eV), and thus $e_g(\uparrow)$ states appear between $t_{2g}(\uparrow)$ and $t_{2g}(\downarrow)$ states (Fig. 2). This means that the Co atom in the HS state, which is Co^{II}(d^7: $t_{2g}^5 e_g^2$, S=3/2). In contrast, the exchange splitting is much smaller in Fe, and thus represents the LS d^5 structure, Fe^{III}(d^5: $t_{2g}^5 e_g^0$, S=1/2). These findings are in agreement with experimental absorption spectra.[12,13]

A range of different long-range magnetic orderings are predicted experimentally.[1,2,18,33] However, it is important to note that the photoinduced reversible spin crossovers in PBAs are local phenomena, and do not depend on the nature of long-range Fe-Co magnetic order. These transitions are observed both below (< 20 K) and well above (> 200 K) the magnetic ordering temperature.[1,2,18] In the present calculation, we find that for $U_{Co/Fe}^{eff}$=3 eV, the ferrimagnetic (FIM) state lies 60 meV higher in energy than the FM state at 0 K. Although ΔE_{LH} depends strongly on the magnitude of the Hubbard U term, the FM to FIM energy difference Δ_{FM-FIM} does not show considerable U dependence. For 3.5 eV

> $U_{Co/Fe}^{eff}$ > 1.5 eV, calculated Δ_{FM-FIM} ranged only 50-60 meV. In contrast, for $U_{Co/Fe}^{eff} \leqslant$ 1.5 eV, calculations do not stabilize the FIM configuration. The long-range Co^{II}-Fe^{III} magnetic interaction exhibits competing FM and antiferromagnetic (AFM) superexchange contributions. The FM contribution exists over two channels, J_{FM}(Co-$e_g^2 \leftrightarrow$ Fe-t_{2g}^5); the AFM contribution exists over one channel, J_{AFM}(Co-$t_{2g}^5 \leftrightarrow$ Fe-t_{2g}^5). Thus, the effective Co-Fe interaction for defect-free CoFe-PBA is predicted to be ferromagnetic. The calculated Δ_{FM-FIM} energy difference is solely attributed to the long-range magnetic orientation as we find the optimized FM and FIM to have identical structural parameters. Moreover, the CT excitation in the FIM state is similar to the FM state, which triggers the transition.

Now let us consider the entire transition mechanism, which is mediated via intermediate states (Fig. 3). We have noted that both the forward and reverse transitions are triggered by metal-to-metal CT excitations, as is evidenced by the local density of states (Fig. 2). This CT excitation is followed by the $d \rightarrow d$ interconversion in the Co center, which completes the spin transition. Although the HS excited state lies only 0.18 eV/fu higher in energy than the LS ground state (Fig. 3), the LS↔HS transitions require much higher energy. This relative energetic cost of the forward and reverse transitions is corroborated by experimental absorption spectra.[1,2,14]

The $|e|$ charge transfer from Fe-t_{2g} states to the dou-

bly degenerate Co-e_g^* state in the first step (Fig. 2) initiates the forward LS→HS transition. However, the subsequent interconversion of the d-electrons does not occur readily, as the HS states for bond lengths $d_{Co-N} < 1.95$ Å are of higher energy than the intermediate state, IS-I (Fig. 3). Calculated metal-to-metal CT excitation energy required for this transition (2.08 eV) agrees reasonably well with the experimental absorption spectra.[1,2,30] The transferred electron in the IS-I state, $Fe^{III}(t_{2g}^5)$-CN-$Co^{II}(t_{2g}^6 e_g^1)$, can occupy either of the degenerate $d_{x^2-y^2}^*$ and $d_{z^2}^*$ states (antibonding σ^* Co-N states), and thus IS-I is strongly Jahn-Teller active. Therefore, the CT excitation in the first step prompts tetragonal JT distortion in the CoN_6 octahedra (elongated along z, and essentially unchanged in x and y). Such distortion lifts the Co-e_g^* degeneracy, and the $d_{z^2}^*$ state moves down in energy monotonically with increasing tetragonal distortion; this decreases Co-N ligand strength along the z-axis. This tetragonal distortion is completed at a bond length of $d_{Co-N}^z \simeq 2.15$ Å. However, the Co-t_{2g} and Co-$d_{x^2-y^2}^*$ states remain unchanged in energy, as the orbitals are oriented at 45° to or are co-linear with the CN ligand in the $x-y$ plane, respectively. Thus, during the tetragonal distortion, the energy gap between the occupied t_{2g} and unoccupied $d_{x^2-y^2}^*$ states remains unchanged around ∼2 eV; this corresponds to the energy of blue light. During this JT distortion (for $d_{Co-N} > 1.95$ Å), the $t_{2g} \to d_{x^2-y^2}^*$ interconversion at the Co center completes the forward spin transition to HS-$Co^{II}(t_{2g}^5 e_g^2)$. Subsequently, the distorted CoN_6 octahedra is relaxed in the $x-y$ plane to remove the JT distortion. The octahedra are thus restored to an undistorted configuration in which the Co-N bond lengths are 0.21 Å longer than those in the LS state (Fig. 1 and Table I).[1,2,12,13]

In the reverse HS→LS transition, the calculated CT excitation of 1.25 eV (Fig. 2) agrees reasonably well with the experimental absorption peak at 1319 nm (0.94 eV).[1,2] The intermediate state IS-II for the reverse transition exhibits the electronic configuration, $Fe(t_{2g}^6)$-CN-$Co(t_{2g}^5 e_g^1)$. Similar to the forward transition, the CT excitation is also followed by $d \to d$ interconversion in the Co center to complete the reverse transition. However, unlike the forward spin transition, the Co $e_g \to t_{2g}$ interconversion does not require JT distortion. In the reverse transition, the LS state is lower in energy than the IS-II state for all bond lengths $d_{Co-N} < 2.10$ Å (Fig. 3). This IS-II state exhibits uniform d_{Co-N} (i.e., is undistorted); in contrast, the JT distorted version of the IS-II is higher in energy. Further, at $d_{Co-N}=2.10$ Å, the unoccupied Co-t_{2g} state is just above the Fermi level and the occupied Co-e_g state is at the Fermi level. Thus, the Co $e_g \to t_{2g}$ interconversion is readily accessible at 2.10 Å after the Co-to-Fe charge transfer. Consequently, the CoN_6 octahedra shrink isotropically to recover the LS lattice constants upon completion of the reverse spin transition (Fig. 1).

These findings also demonstrate that water molecules within PBAs are not an essential prerequisite to trigger the spin transitions. The CT excitation energies, which were calculated in the absence of H_2O, are in good agreement with the experimental absorption spectra for PBA samples that contained various levels of H_2O content. Thus, we posit that H_2O negligibly affects the CT excitation in PBAs. This expectation is supported by the recent findings of Wojdeł, who calculated CT excitation energies for $KFe[Fe(CN)_6]$ with and without H_2O, and found these to differ only by 0.2 eV.[23] In contrast, previous simulations of PBA clusters (rather than crystals) were interpreted to posit a significant and essential role of H_2O in PBA spin transitions.[19] Thus, our current findings are in better agreement with available experiments and with recent calculations for anhydrous and water-containing Prussian blue crystals in the LS state.[23] This correspondence is due ostensibly to the fact that we have modeled the actual crystal and found the crystal symmetry distortion to couple strongly to the spin transition mechanisms.

Further, we note that such spin transitions can be induced by hydrostatic pressure,[34,35] as the electronic excitations are strongly coupled with the internal PBA lattice dimensions. For the HS state, external compressive stress destabilizes the Co-e_g^* antibonding states, because the ligand strength increases as CN^- ligands move toward the Co center. We find that at ∼3 GPa pressure ($a \simeq 10.20$ Å, $d_{Co-N} \simeq 2$ Å) the LS (low T) phase becomes more stable than the HS phase. This finding points toward one novel route by which the spin state, color, and other physical properties of PBAs may be induced by mechanical rather than electromagnetic stimuli.

IV. CONCLUSIONS

We demonstrate through *ab initio* PBE+U calculations that the repeatable and reversible photoinduced spin crossover in CoFe-PBA is driven by metal-to-metal charge transfer. This charge transfer is followed by $d \to d$ interconversion at the Co center. In agreement with experimental observations, these spin transitions are strongly coupled with the PBA lattice via CoN_6 octahedra,[1,2,12,13] which in turn tune the ligand field splitting. We find that the LS→HS transition requires an intermediate, tetragonal Jahn-Teller distortion of the CoN_6 octahedra. Moreover, the calculated charge transfer excitations show that H_2O is not an absolute prerequisite to trigger the spin transition. Although we have studied the CoFe-PBA here, including the mechanical analogue to electromagnetic spin transition induction, the proposed mechanisms are anticipated to be similar for the large class of Prussian blue analog materials.

ACKNOWLEDGMENTS

[1] O. Sato, T. Iyoda, A. Fujishima, and K. Hashimoto, Science, **272**, 704 (1996).

[2] O. Sato, Y. Einaga, T. Iyoda, A. Fujishima, and K. Hashimoto, J. Electrochem. Soc., **144**, L11 (1997).

[3] C. Bressler, C. Milne, V.-T. Pham, A. ElNahhas, R. M. van der Veen, W. Gawelda, S. Johnson, P. Beaud, D. Grolimund, M. Kaiser, C. N. Borca, G. Ingold, R. Abela, and M. Chergui, Science, **323**, 489 (2009).

[4] D. A. Pejaković, C. Kitamura, J. S. Miller, and A. J. Epstein, Phys. Rev. Lett., **88**, 057202 (2002).

[5] J.-W. Yoo, R. S. Edelstein, D. M. Lincoln, N. P. Raju, and A. J. Epstein, Phys. Rev. Lett., **99**, 157205 (2007).

[6] J.-F. Lin, V. V. Struzhkin, S. D. Jacobsen, M. Y. Hu, P. Chow, J. Kung, H. Liu, H.-k. Mao, and R. J. Hemley, Nature (London), **436**, 377 (2005).

[7] M. Takano, S. Nasu, T. Abe, K. Yamamoto, S. Endo, Y. Takeda, and J. B. Goodenough, Phys. Rev. Lett., **67**, 3267 (1991).

[8] H. Hsu, P. Blaha, M. Cococcioni, and R. M. Wentzcovitch, Phys. Rev. Lett., **106**, 118501 (2011).

[9] J. A. Real, E. André, M. C. Muñoz, M. Julve, T. Granier, A. Bousseksou, and F. Varret, Science, **268**, 265 (1995).

[10] Y. Qi, E. W. Mller, H. Spiering, and P. Gtlich, Chem. Phys. Lett., **101**, 503 (1983).

[11] T. Ikeue, Y. Ohgo, T. Yamaguchi, M. Takahashi, M. Takeda, and M. Nakamura, Angew. Chem. Int. Ed., **40**, 2617 (2001).

[12] T. Yokoyama, T. Ohta, O. Sato, and K. Hashimoto, Phys. Rev. B, **58**, 8257 (1998).

[13] T. Yokoyama, M. Kiguchi, T. Ohta, O. Sato, Y. Einaga, and K. Hashimoto, Phys. Rev. B, **60**, 9340 (1999).

[14] H. W. Liu, K. Matsuda, Z. Z. Gu, K. Takahashi, A. L. Cui, R. Nakajima, A. Fujishima, and O. Sato, Phys. Rev. Lett., **90**, 167403 (2003).

[15] S. Koshihara, Y. Tokura, K. Takeda, and T. Koda, Phys. Rev. Lett., **68**, 1148 (1992).

[16] J.-D. Cafun, G. Champion, M.-A. Arrio, C. C. dit Moulin, and A. Bleuzen, J. Am. Chem. Soc., **132**, 11552 (2010).

[17] A. Bleuzen, J.-D. Cafun, A. Bachschmidt, M. Verdaguer, P. Munsch, F. Baudelet, and J.-P. Itie, J. Phys. Chem. C, **112**, 17709 (2008).

[18] D. A. Pejaković, J. L. Manson, J. S. Miller, and A. J. Epstein, Phys. Rev. Lett., **85**, 1994 (2000).

[19] T. Kawamoto, Y. Asai, and S. Abe, Phys. Rev. Lett., **86**, 348 (2001).

[20] K. Kato, Y. Moritomo, M. Takata, M. Sakata, M. Umekawa, N. Hamada, S. Ohkoshi, H. Tokoro, and K. Hashimoto, Phys. Rev. Lett., **91**, 255502 (2003).

[21] D. Papanikolaou, S. Margadonna, W. Kosaka, S.-i. Ohkoshi, M. Brunelli, and K. Prassides, J. Am. Chem. Soc., **128**, 8358 (2006).

[22] J. C. Wojdeł, I. de P. R. Moreira, and F. Illas, J. Chem. Phys., **130**, 014702 (2009).

[23] J. C. Wojdeł, J. Mol. Model., **15**, 567 (2009).

[24] J. P. Perdew, K. Burke, and M. Ernzerhof, Phys. Rev. Lett., **77**, 3865 (1996).

[25] P. E. Blöchl, Phys. Rev. B, **50**, 17953 (1994).

[26] G. Kresse and J. Hafner, Phys. Rev. B, **47**, 558 (1993).

[27] G. Kresse and J. Furthmüller, Phys. Rev. B, **54**, 11169 (1996).

[28] C. Adamo and V. Barone, J. Chem. Phys., **110**, 6158 (1999).

[29] D. S. Middlemiss and C. C. Wilson, Phys. Rev. B, **77**, 155129 (2008).

[30] K. Igarashi, F. Nakada, and Y. Moritomo, Phys. Rev. B, **78**, 235106 (2008).

[31] V. Escax, G. Champion, M.-A. Arrio, M. Zacchigna, C. Cartier dit Moulin, and A. Bleuzen, Angew. Chem. Int. Ed., **44**, 4798 (2005).

[32] S. Bonhommeau, N. Pontius, S. Cobo, L. Salmon, F. M. F. de Groot, G. Molnár, A. Bousseksou, H. A. Dürra, and W. Eberhard, Phys. Chem. Chem. Phys., **10**, 5882 (2008).

[33] S. Juszczyk, C. Johansson, M. Hanson, A. Ratuszna, and G. Malecki, J. Phys.: Cond. Mat., **6**, 5697 (1994).

[34] V. Ksenofontov, G. Levchenko, S. Reiman, P. Gütlich, A. Bleuzen, V. Escax, and M. Verdaguer, Phys. Rev. B, **68**, 024415 (2003).

[35] Y. Moritomo, M. Hanawa, Y. Ohishi, K. Kato, M. Takata, A. Kuriki, E. Nishibori, M. Sakata, S. Ohkoshi, H. Tokoro, and K. Hashimoto, Phys. Rev. B, **68**, 144106 (2003).